

We are IntechOpen, the world's leading publisher of Open Access books Built by scientists, for scientists

4,800

Open access books available

122,000

International authors and editors

135M

Downloads

Our authors are among the

154

Countries delivered to

TOP 1%

most cited scientists

12.2%

Contributors from top 500 universities



WEB OF SCIENCE™

Selection of our books indexed in the Book Citation Index
in Web of Science™ Core Collection (BKCI)

Interested in publishing with us?
Contact book.department@intechopen.com

Numbers displayed above are based on latest data collected.
For more information visit www.intechopen.com



Coexistence of Bipolar and Unipolar Memristor Switching Behavior

Sami Ghedira, Faten Ouaja Rziga, Khaoula Mbarek and Kamel Besbes

Abstract

The memristor has been theoretically investigated as one of the fundamental electrical elements by Pr. Leon Chua in 1971. Meanwhile, its electrical characteristics are not yet fully understood. The nonlinear characteristics and the ability to examine large-scale amounts of storing data of this device reveal an interesting development in emerging electronic systems. Research on memristor modeling based on SPICE tools has grown rapidly. This leads us to study the behavior of such devices. Our aim is to simulate different types of memristor behavior. The adjustment of the model is based on the implementation of several parameters, which enables the switching of this device. In this chapter, we prove the flexibility and the correlation of memristor model with different memristive characterization data, by applying different voltage bias, sinusoidal and with a repetitive sweeping. Moreover, we demonstrate the memristor behavior as four types of switching. This includes bipolar switching, unipolar switching, bipolar switching with forgetting effect, and a reversible process between bipolar and unipolar switching. In order to validate this study, we compare our simulation results with experimental data and we prove a good agreement. The SPICE model used in our simulations shows a special advantage for its flexibility and simplicity.

Keywords: memristor, I-V characteristics, SPICE model, switching behavior, hysteresis loop, bipolar behavior, unipolar behavior

1. Introduction

Significant interest has been focused on the development of memristor-based systems. It has been first developed on symmetry consideration by Prof. Leon Chua in 1971 [1, 2]. In addition, it has been admitted physically by the HP Labs Team in 2008 [3]. This device does have a great potential to be the future memory cell, due to the small feature size and ability to retain the content (nonvolatile). The identity of such device is obvious on the I - V characteristics, i.e., its “pinched hysteresis loop.” Thus, the choice of the model and the structure are necessary to achieve

better endurance and performance. Hence, the correlation of one model to other memristive devices is an interesting development to further research.

In the literature, memristor models studied in [3–10] have been published for basic mathematical functioning properties of the memristor, which have been proposed by HP Labs in [3]. Other models [11–14] focus on extracting the I - V characteristic of the model with other mathematical method using boundary conditions. They differ in complexity, materials, and accuracy. Thus, since our interest is in the behavior of the memristor, we choose to explore and investigate a simple SPICE model, which has been proposed by the present authors in [11]. The main differences are displayed in the implementation of parameters such as the state variable of the device. However, so far, no SPICE model could be correlated to several characterizations data of memristive devices. Our goal is to use a memristor model to analyze its functioning for different voltage bias. We study the dynamical behavior of memristor and we demonstrate that this model accounts for four different types of a memristor cited as the following: the bipolar behavior of memristor, the unipolar behavior, the bipolar with forgetting effect, and the reversible process between the bipolar and the unipolar behavior of memristor. Those types of memristor change under distinct stimulus such as sinusoidal, triangular, and repetitive DC sweeping voltage.

2. Theoretical principles

The wide variety in memristor structure and composition has led to the development of many different memristor modeling techniques. Some of them have been designed to represent a specific device for a specific type of application, such as AHaH [12], ANN [15, 16], Slime mold [17], and neuromorphic applications [5]. Implementation of the memristor could be generated on several tools of simulation, such as SPICE [18–25], Matlab [26–32], Verilog-A [33], and VHDL-AMS [34–37]. Resistive switching behavior is one of the fundamental properties showed in memristors; the well-known HP lab model of a memristor [3] shown in **Figure 1(a)** consists of a thin TiO_2 double-layer of width D between a pair of platinum

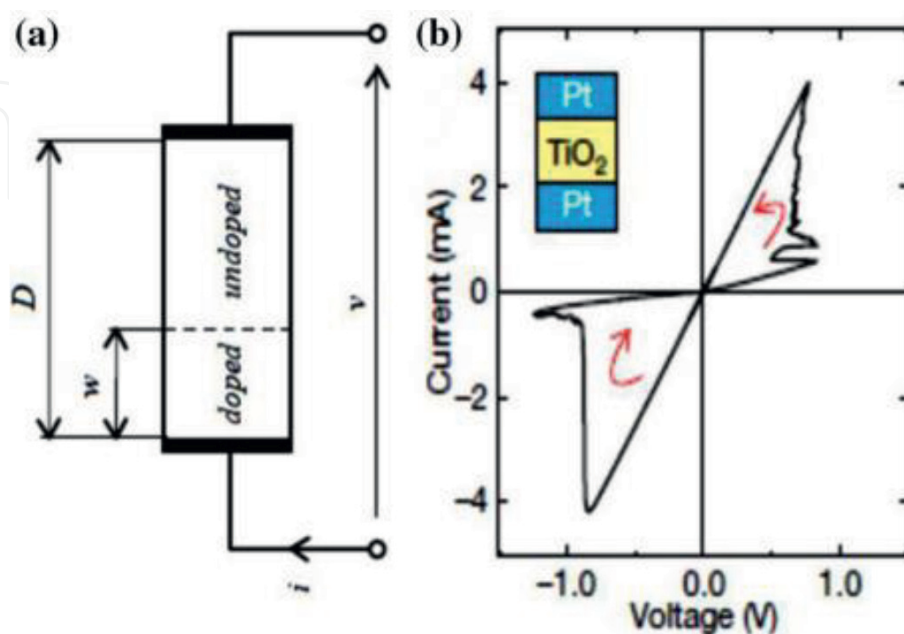


Figure 1. Physical model of memristor [3]. (a) Memristor thin film. (b) Memristor hysteresis loop.

electrodes. One of the TiO_2 layers of width w is doped with oxygen vacancies. The second, undoped layer of width $w-D$ has insulating properties. As a result of complex processes in the device, the width w of the doped layer varies by applying a voltage or current to the electrodes of the memristor, and there will be dramatic changes in resistance. Therefore, the boundary, defined as the state variable $x = w/D$, between the two layers moves simultaneously. The well-known characteristic of the memristor is shown in **Figure 1(b)**, the pinched hysteresis loop, which indicates the switching behavior of memristive devices. An application of a positive bias voltage to the electrodes of the device leads to the switching between Off and On states, and this switching is labeled SET. A RESET switching corresponds to the exchange between On and Off states. As current flows through the device, the cross section between the regions moves. As a result, the doped and the undoped regions have resistance R_{on} and R_{off} when each of them reaches the $(D-w)$ and the full-length D , respectively. Also, the width w of the doped region of the memristor increases by applying a positive voltage bias, which causes the total resistance of the device to decrease. The same process is carried out by applying a negative voltage to the opposite side of the device. Moreover, there are two methods of the behavior of resistive switching for memristors: static and dynamic switching.

2.1 Static characteristics

The characteristic of a static switching behavior is obtained with a slow sweep of the voltage applied to the terminals of the device between the minimum and maximum values eligible (typically a triangular signal).

2.2 Dynamic characteristics

In dynamic switching, voltage pulses are applied to the device and the current rises under the constant voltage bias during the pulsing interval.

A comprehensive mathematical illustration of a SPICE memristor model has been reported in [11], which will be used later on for our simulation results. This model can illustrate the static and dynamic switching behavior, which will be studied in the next section. Thus, this model is based on the assumption that the switching behavior of the memristor is small or fast, below or above a threshold voltage V_{SET} or V_{RESET} , respectively, which is considered as the minimum voltage required to impose a change on the physical structure and thus the memristance of the device. This assumption is encapsulated in the use of the multiple implemented parameters, which are included in the set of equations below:

$$I(t) = \begin{cases} a_1 x(t) \sinh(bV(t)), & V(t) > 0 \\ a_2 x(t) \sinh(bV(t)), & V(t) < 0 \end{cases} \quad (1)$$

The relationship between the memristor voltage and the memristor current is given by Eq. (1), and it comprises three main parameters: a_1 , a_2 , and b . These parameters are responsible for the modeling of the nonlinear phenomenon of the pinched hysteresis loop. a_1 and a_2 are the magnitude parameters that vary according to the polarity of the input voltage; it is also related to the thickness of the dielectric layer of the memristor. Meanwhile, b is defined as the control parameter, which refers to the amount of oxygen deficiencies presented in the device, and it controls the conductivity of the device. The main voltage equation is defined by the relation $g(t)$ defined below:

$$g(t) = \begin{cases} A_p (e^{V(t)} - e^{V_p}), & V(t) > V_p \\ -A_n (e^{-V(t)} - e^{V_n}), & V(t) < -V_n \\ 0, & -V_n \leq V(t) \leq V_p \end{cases} \quad (2)$$

Equation (2) incorporates the threshold voltage with V_p and V_n which refers to the positive and negative polarizations, respectively, which makes a change in the switching behavior for value below the external voltage of the memristor. A_p and A_n are fitting parameters that affect the conductivity of the device. Accurately, it controls the speed of the oxygen deficiencies motion. The demonstration of the linearity of the model is described by parameters included in the following equations:

$$f(x) = \begin{cases} e^{-\alpha_p(x-x_p)} w_p(x, x_p), & x \geq x_p \\ 1, & x < x_p \end{cases} \quad (3)$$

$$f(x) = \begin{cases} e^{\alpha_n(x+x_n-1)} w_n(x, x_n), & x \leq 1 - x_n \\ 1, & x > 1 - x_n \end{cases} \quad (4)$$

The physical parameters x_p and x_n have been defined in Eqs. (3) and (4); it represents the value of the state variable, which is responsible for the linearity of the device. Fitting parameters α_p and α_n are also included in these equations; are responsible for the linearity of the device; and they determine the degree of motion including the amortization of the state variable. The parameters w_n and w_p are defined by Eqs. (5) and (6), respectively. Those functions are used to shape the intensity of the state variable dynamics, i.e., the rate of memristance change.

$$w_p(x, x_p) = \frac{x_p - x}{1 - x_p} + 1 \quad (5)$$

$$w_n(x, x_n) = \frac{x}{1 - x_n} \quad (6)$$

Equation (7) represents the modeling function of the state variable. The fitting parameter η represents the direction of the movement of the state variable depending on the polarity of the input voltage. When $\eta = 1$, a positive voltage greater than the threshold voltage will increase the value of the state variable; and when $\eta = -1$, a positive voltage will decrease the value of the state variable.

$$\frac{dx}{dt} = \eta g(V(t)) f(x(t)) \quad (7)$$

Each pair of the parameters indicates the variation in the positive and negative region of the polarization. These multiple parameters make it possible for this device to be adaptable to a variety of characterization data of memristive devices, which we will discuss in the next section.

3. Analysis of the I - V characteristics

In our previous work [38], we illustrated a methodology for a simple memristor model to automatically adjust other behaviors of memristive devices. It effectively

demonstrates the basic I - V characteristics of a memristive device. In addition, it acts differently in the positive and negative regions of the applied voltage, and the implemented parameters of the device take account on this, which makes the analysis of the pinched hysteresis loop simple and coherent for the positive and the negative regions independently. Therefore, we analyze the fundamental fingerprint of the macromodel and its memristance switching behavior. In the simulation results of **Figure 2(a)**, we used a sinusoidal voltage 0.46 V with a frequency of 100 Hz, **Figure 2(b)** shows the resultant pinched hysteresis loop, which correlates the characterization data of the proposed model [11]. Thereby, our results agree well with the experimental results already published in [11], and we prove the linearity property of the device for a higher value of frequency. The next simulation results reveal the richness of memristor's switching behavior confirming the usefulness of the specific design approach. The effect of memristive switching is inspected by varying the implemented parameters of the model such as the magnitude of the voltage bias, the initial charge, and the state variable.

This changes the operating regime so the memristance value may not remain constant and the memristor operates in different segments or takes different memristance values. This sudden jump of memristance is called “memristive switching” or “resistive switching.”

In this case, memristive switching depends on the bias of the applied voltage across the device, which is represented in **Figure 3(a)**, the curve of the state variable motion at memristor boundaries. We consider the memristor in an Off state, as an initial state of the device, switching the device to On state, requires a positive bias across the device. While switching it to Off state requires negative bias.

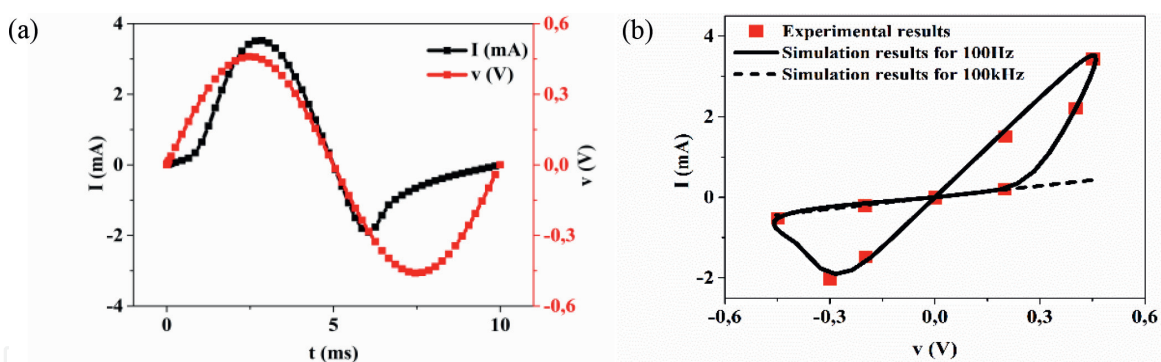


Figure 2. (a) Curve of current and voltage applied to the terminals of the memristor. (b) Represents the resultant hysteresis loop at 100 Hz and 100 kHz where the deviates linear.

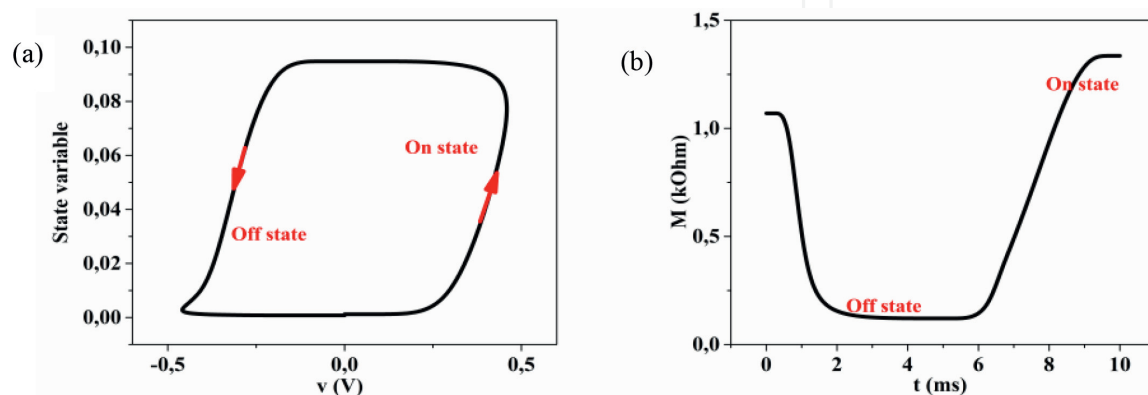


Figure 3. (a) The state variable motion at memristor boundaries according to the applied voltage and (b) memristance behavior over time.

Figure 3(b) represents the curve of the memristance or the resistance of the memristor on the On and Off states. From this results, R_{on} and R_{off} 's value estimated by $1.3\text{ k}\Omega$ and $1.1\text{ k}\Omega$, respectively.

4. Correlation of different memristive devices

In this section, we present our simulation results, in which we implement the different values of parameters on PSPICE, to fit a set of memristive devices studied for different types of applications. Those results describe the static and dynamical characteristics of the model. Thus, we prove that the SPICE model fits well with the characterization data of memristors defined in [8, 15, 17, 25, 39–44]. The polarization voltages studied are either sinusoidal pulses or repetitive DC sweeping voltage to represent the different switching resistive levels of the memristor. The simulation results of the proposed model [11] shown in **Figure 4**, which indeed shows the characterization data of several memristive devices. In these simulation results, we adjust the different implement parameters on the SPICE model to fit the experimental results presented in [11]. Thus, it describes the I - V characteristics for devices defined in [8, 9, 40–43], which has been correlated by the SPICE model.

- a. **Figure 4(a)** describes the simulation results of the device published by the State University of Boise in [40].
- b. **Figure 4(b)** describes the simulation results of the device published by the Tel Aviv University in [9, 41].
- c. **Figure 4(c)** describes the simulation results of the device published by the University of Michigan in [8].
- d. **Figure 4(d)** describes the simulation results of the device published by the state University of Iowa in [42].
- e. **Figure 4(e)** describes the simulation results of the device published by the University of Michigan in [43].

4.1 Memristive device of the laboratory of slime mold

We adjust the implemented parameters to find the appropriate shape of I - V characteristics of the Slime mold device [17] shown in **Figure 5**, our results fits well the experimental results described in [17]. The application of Slime mold is a group of bacteria that lives mainly in the soil, which has the ability to change its shape by sliding every 50 s (by extension and retraction). This outcome contributes to the development of bioelectronics circuits of self-growth. The I - V characteristics curve for a DC voltage and a repetitive sweeping and the curve of the resistance of the device shown in **Figure 5(a)–(c)**, respectively. These results present the functionality of this model by applying a repetitive DC sweeping voltage to present the various resistance switching states.

4.2 Memristive device of Strachan of the HP laboratory

Another memristive device based on TaO_x was proposed by the team of HP Labs in [44]; we adjust the fitting parameters with the characterization data of this

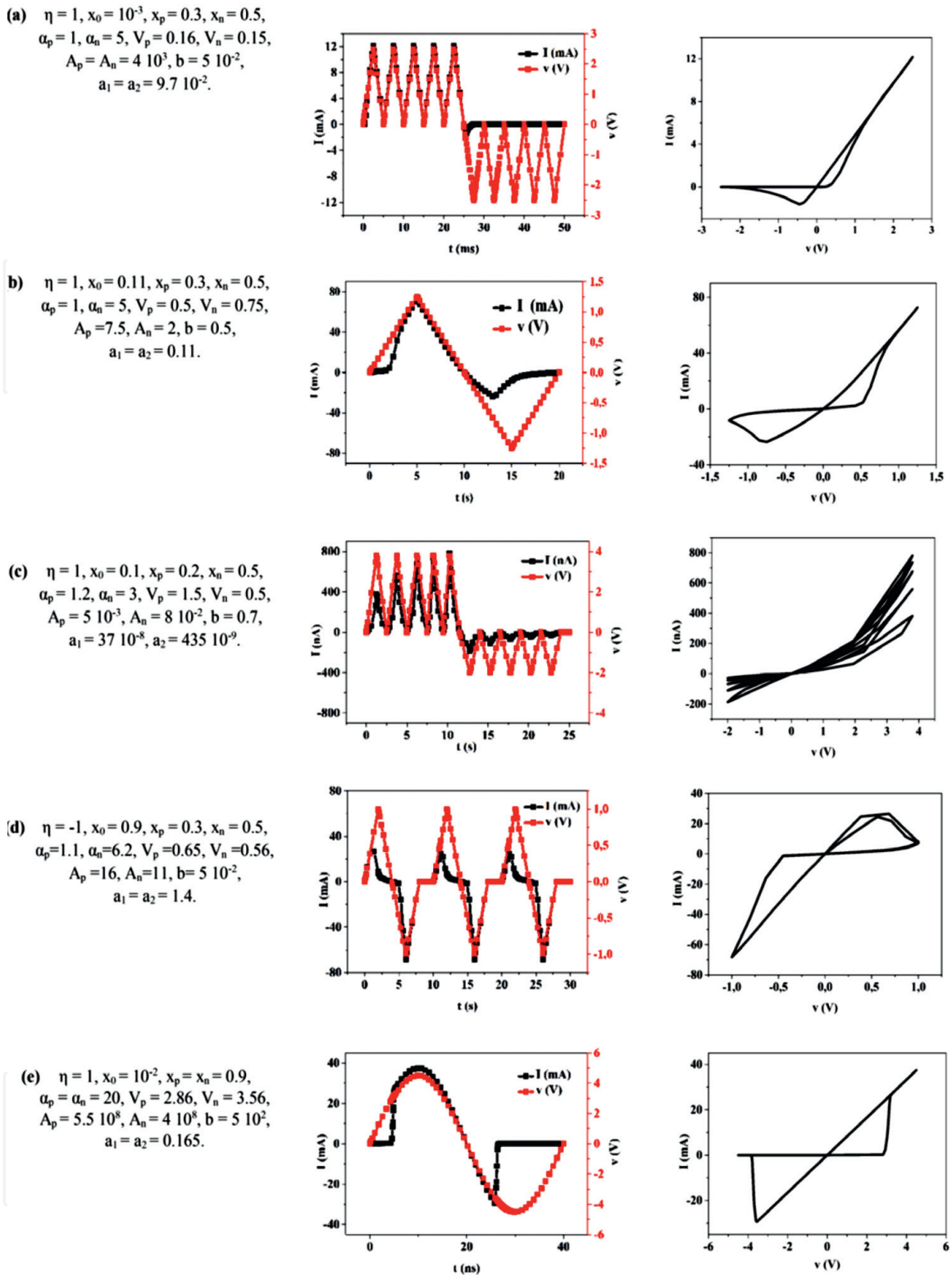


Figure 4. (a) I-V curve of memristive device proposed by the State University of Boise [40], (b) I-V curve of memristive device proposed by the Tel Aviv University [41], (c) I-V curve of memristive device proposed by the University of Michigan in 2010 [8], (d) I-V curve of the device proposed by the State University of Iowa in 2010 [42], and (e) I-V curve of the device proposed by the University of Michigan [43] including the parameter values.

device. The results are shown in **Figure 6**; it agrees with the experimental results represented in [44]. The I-V characteristic curve for a DC voltage and a repetitive sweeping and the curve of the resistance of the device are shown in **Figure 6(a)–(c)**, respectively. The simulation results present the functionality of this model by applying a repetitive DC sweeping voltage to present the several resistance switching states.

4.3 Memristor of Nugent for AHaH applications

Our model also fits well a learning AHaH application accomplished by Nugent in [12]. After the application of a sinusoidal signal to the memristor with amplitude 0.25 V for a period 10 ms, we found the resultant I - V characteristics shown in **Figure 7(a)**, which seems compatible with the I - V characterization profile and it fits well the experimental results revealed in [12]. This model works well for a repetitive DC sweeping voltage which is represented by the I - V characteristics curves and the curve of the resistance of the device shown in **Figure 7(b), (c)**. The simulation results present the functionality of this model by applying a repetitive DC sweeping voltage to present the several resistance switching states.

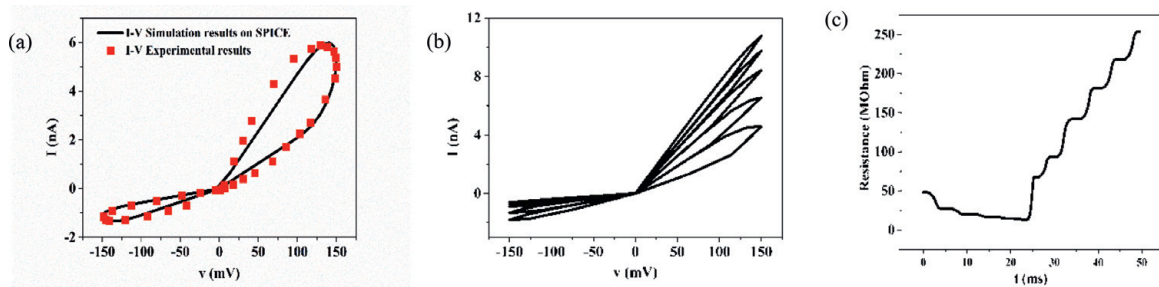


Figure 5.

Simulation results of the memristor model adapted to the I - V characteristics profile of Slime mold memristive device, the Simulation value: $\eta = 1$, $x_0 = 0.11$, $x_p = 0.35$, $x_n = 0.55$, $\alpha_p = 1$, $\alpha_n = 5$, $V_p = 0.1$, $V_n = 0.1$, $A_p = A_n = 4 \cdot 10^3$, $b = 2 \cdot 10^{-5}$, $a_1 = a_2 = 17 \cdot 10^5$.

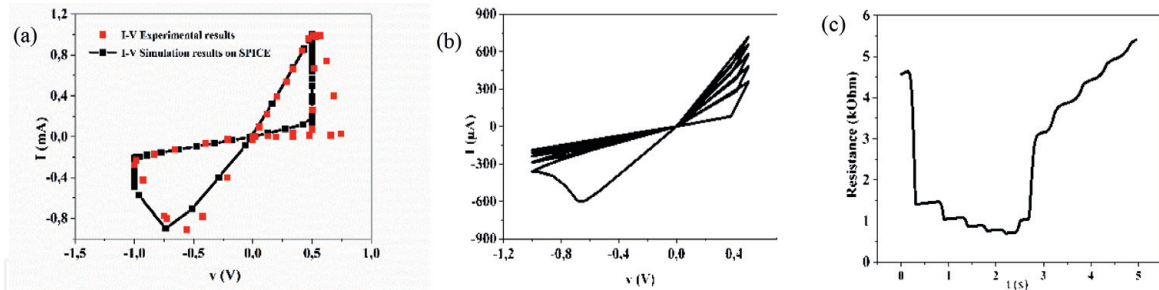


Figure 6.

Simulation results of the model adapted to the I - V characteristics profile of the memristive device of Strachan, the simulation value: $\eta = 1$, $x_0 = 99 \times 10^{-3}$, $x_p = 0.3$, $x_n = 0.63$, $\alpha_p = 0.1$, $\alpha_n = 20$, $V_p = 0.49$, $V_n = 0.6$, $A_p = 400$, $A_n = 25$, $b = 1.3 \times 10^{-3}$, $a_1 = 1.7$, $a_2 = 1.2$.

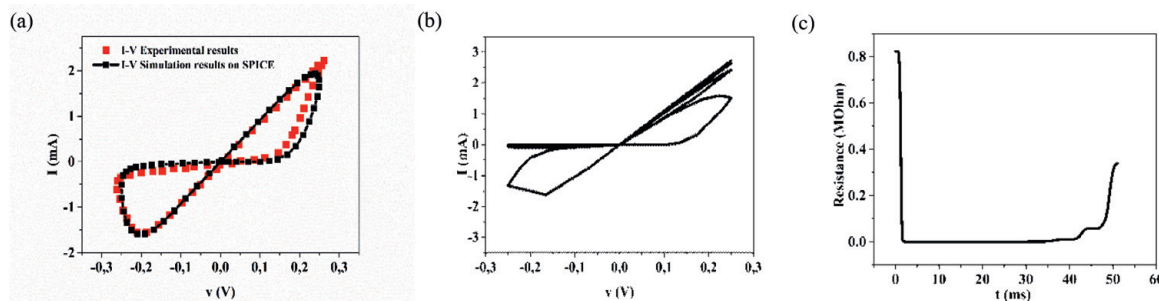


Figure 7.

Simulation results of the model adapted to the I - V characteristics profile of the memristive device of Nugent, the simulation value: $\eta = 1$, $x_0 = 1.1 \times 10^{-4}$, $x_p = 0.3$, $x_n = 0.8$, $\alpha_p = 1$, $\alpha_n = 5$, $V_p = 0.1$, $V_n = 0.13$, $A_p = A_n = 4 \times 10^3$, $b = 6.5 \times 10^{-2}$, $a_1 = a_2 = 0.17$.

4.4 Memristive device of the University of Pittsburgh

The device represented by Zhang in [39] is based on TaO_x material. The simulation results of this device are represented in **Figure 8(a)** by applying a triangular voltage with a sweeping of the magnitude, 0.74 V for the positive region, and -1.25 V for the negative region. After adjustment of the parameters, we have a nonlinear I-V curve which seems to be compatible with the I-V characterization profile recorded in the experiments of HP labs in [39]. In addition, we proved the functioning of this device with a repetitive DC sweeping voltage to present several resistance switching states shown in **Figure 8(b)** and (c).

4.5 Memristive device for ANN learning application

Meanwhile, we also simulated the model with a square wave excitation shown in **Figure 9**. This excitation method is used as a learning method, which presents the behavior of this model as an artificial neural network ANN [15]. We follow the learning experience carried out in [16]. As shown in **Figure 9(c)**, the memristance of the device increases along with the applied voltage. However, this behavior response is different from the other previous excitation, and this depends on the type of excitation and the followed current. The current curve decreases with each pulse of the excitation voltage positive and negative.

In conclusion, we notice that this SPICE model is a general model that can be applied in multiple domains. Furthermore, according to the simulation results of both devices Slime mold and HP Labs, we notice that the hysteresis loop of the memristor maintains its nonlinear shape even for a remarkable range of the values of the parameters. The speed of movement for the memristive devices of Slime mold and Nugent are faster compared to the other memristive devices since A_p and

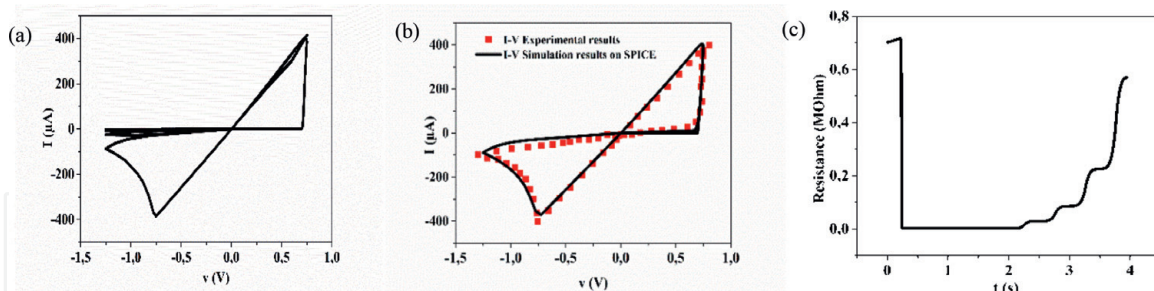


Figure 8. Simulation results compared to the simulation result of Zhang, the simulation value: $\eta = 1$, $x_o = 55 \times 10^{-4}$, $x_p = 0.32$, $x_n = 0.1$, $\alpha_p = 1$, $\alpha_n = 5$, $V_p = 0.7$, $V_n = 0.75$, $A_p = 4 \times 10^3$, $A_n = 500$, $b = 11 \times 10^{-4}$, $a_1 = 0.17 \times 10^3$, $a_2 = 1.1 \times 10^3$.

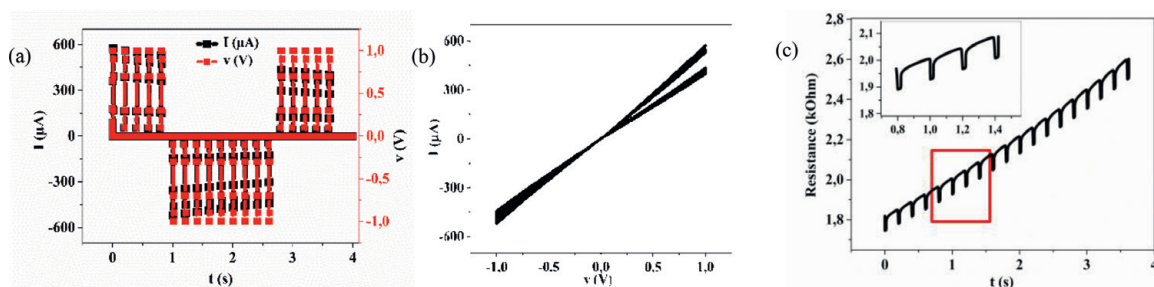


Figure 9. Simulation results of the model adapted to learning application, the simulation value: $\eta = 1$, $x_o = 0.11$, $x_p = 0.3$, $x_n = 0.5$, $\alpha_p = 1$, $\alpha_n = 5$, $V_p = V_n = 1$, $A_p = A_n = 4$, $b = 0.5$, $a_1 = a_2 = 0.01$.

A_n have higher values. Thus, the memristive devices of Slime mold and Zhang application have the lowest values of b , which decrease its conductivity. The ANN learning application presents another type of excitation, which largely affects the dynamic of the memristor's behavior. Thus, we will deal later with the use of different memristor switching behavior, we demonstrate not only bipolar, but also the unipolar switching behavior of memristors, which differs from bipolar memristors in the fact that only the magnitude of the voltage across the device determines the change in the resistance.

5. Behavior of the SPICE model for different types of memristors

Memristor models, in literature, have different responses, which are generated for four different types of a memristor, i.e., bipolar, bipolar with a forgetting effect, unipolar and reversible behavior between the bipolar, and the unipolar memristor. For our simulation results, we used a SPICE model that can not only describe the basic memory ability of memristor, but also be able to capture all of the four types of memristor switching behavior.

Models with bipolar switching [45, 46] distinguishable by the memristance which increases and decreases by different polarity voltages. Models with unipolar switching behavior [45, 46] are distinguishable by its memristance, which can increase and decrease by the same polarity voltage. The bipolar with forgetting effect [47, 48] is distinguishable by its memristance which increases and decreases by a different polarity voltage, but memristance can spontaneously decrease at the same time, even with no voltage applied. The reversible bipolar and unipolar switching behavior [49], here the memristor will behave like a bipolar memristor at first, but after a few iterations, it will turn to a unipolar memristor.

In the same context, we use different polarization voltages, either sinusoidal or repetitive DC sweeping voltage, exploited in order to present the different states of resistance of the memristor, and thus it shows the behavior of the four different types of a memristor. Those results reveal the richness of memristor's dynamical behavior confirming the usefulness of the specific model approach.

To verify the memristive characteristics and the coexistence of different switching behavior of our proposed model, we employed different excitations presented in the following figures of the rest of the paper. In fact, to characterize different types of memristors, we need to verify the behavior of the model for the well-known fundamental switching behavior in both bipolar and unipolar switching behavior. In this case, we have adapted our model according to the experimental results demonstrated in [50]. These observations are consistent and in very good qualitative agreement with the experimental results of the memristor switching behavior already published in [50].

In addition, **Figure 10** shows the dynamical characteristics of a bipolar memristor behavior. The sweeping voltage bias approaches a set value $v = 1.8$ V

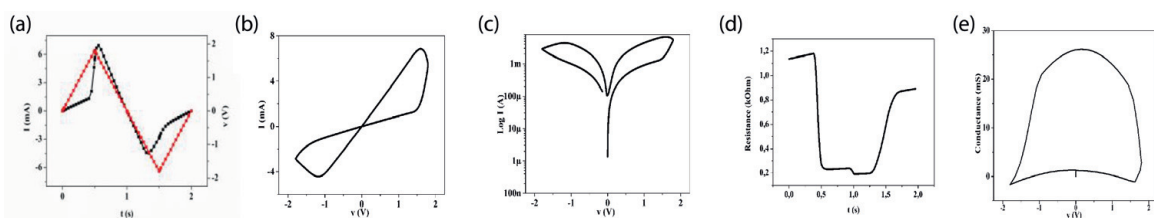


Figure 10.
Memristor SPICE model response for a bipolar switching behavior.

with current value $I = 7 \text{ mA}$. Reversing the voltage polarity, the device switches to a reset value at $v = -1.8 \text{ V}$ with current value $I = -4.5 \text{ mA}$. The attained pinched hysteresis I - V curves are shown in **Figure 10(b)**, **(c)**, which are the typical fingerprint of bipolar resistive switching. The corresponding resistance response is illustrated in **Figure 10(d)**, which was measured according to voltage sweeping with a maximum value of $1.2 \text{ k}\Omega$ and a lower value of $0.9 \text{ k}\Omega$ in the negative and positive voltage application respectively. In addition, **Figure 10(e)** confirms that hysteresis takes place in both I - V and C - V relationships of the device, and it shows a closed switching cycle in the bipolar switching behavior for a maximum value of 25 mS .

Memristor behavior for a bipolar switching with forgetting effect is shown in **Figure 11**. An obvious overlap of the I - V curve is shown in **Figure 11(b)**, **(c)**, due to the repetitive sweeping of the applied voltage. The sweeping voltage bias approaches a set value $v = 1.2 \text{ V}$ with a maximum current value $I = 6 \text{ mA}$. Reversing the voltage polarity, the device switches to a reset value at $v = -1.2 \text{ V}$ with a maximum current value $I = -5 \text{ mA}$. Also, it can be seen from these curves, an accumulation of the current on each pulse. The corresponding resistance response is illustrated in **Figure 11(d)**, which was measured according to voltage sweeping with a maximum value of $1.8 \text{ k}\Omega$ decreasing to a lower value of $0.3 \text{ k}\Omega$ in the positive voltage application, on the opposite side of the negative voltage application the resistance response shows an increase from 0.3 to $0.9 \text{ k}\Omega$. The curve in **Figure 11(e)** shows five switching cycles for a maximum value of 35 mS . This C - V curve shows that the memristance not only increases and decreases by a different polarity voltage, but it also can spontaneously decrease at the same time, even with no voltage applied, and this is a unique switching behavior of memristor. In fact, these curves show the operation of the model as a bipolar memristor with forgetting effect.

Furthermore, the simulation results for the unipolar behavior of memristor are shown in **Figure 12**, which show that another switching behavior is characterized by the memory devices and also that the memristance of the device can increase and decrease by the same polarity of the voltage. For this type of memristor, we use a positive voltage excitation for a value of 2 V and maximum current value $I = 17 \text{ mA}$, which is shown in the curve (**Figure 12(a)**), we notice a slight accumulation of the current on each pulse. The characteristics shown in **Figure 12(d)**, **(e)** describe the resistance and the conductance curve of the memristor. The resistance was

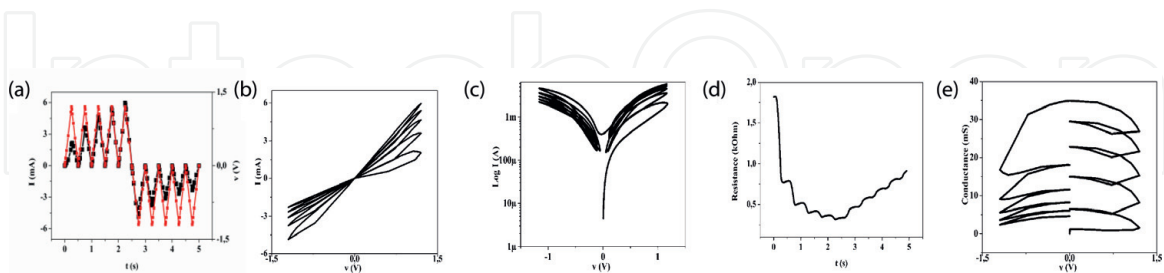


Figure 11.
 Memristor SPICE model response to a bipolar with forgetting effect.

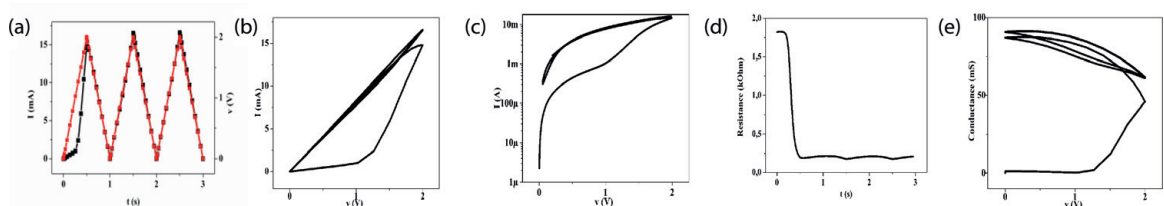


Figure 12.
 Memristor SPICE model response to a unipolar behavior switching.

measured with a maximum value of $2.8 \text{ k}\Omega$ decreasing to a lower value of $0.25 \text{ k}\Omega$. However, the conductance curve (**Figure 12(e)**) shows three switching cycles related to voltage sweeping for a maximum value of 80 mS . In fact, this C - V curve shows that the conductance change in response to three positive pulses, it initially increases (during each pulse stimulus) and subsequently decays toward its original value (between stimuli).

In the end, we represent the results of memristor under a reversible state between the bipolar and the unipolar behavior in **Figure 13**. The sweeping voltage bias, shown in **Figure 13(a)**, approaches a set value $v = 5 \text{ V}$ with a maximum current value $I = 60 \text{ mA}$. Reversing the voltage polarity, the device switches to a reset value at $v = -5 \text{ V}$ with a maximum current value $I = -10 \text{ mA}$.

An obvious overlap of the I - V curve in **Figure 13(b)**, (c) occurs due to the repetitive sweeping of the applied voltage. The corresponding resistance response is illustrated in **Figure 13(d)**, which occurs in a different switching behavior; the rise and fall of the resistance exist but with a large gap between high and low values. The conductance curve in **Figure 13(e)** shows four switching cycles for a maximum value of 100 mS . This C - V curve shows that the first cycle of the switching behavior differs to the other cycles of the switching behavior of the memristor. In fact, the first cycle that can be seen from these curves shows bipolar operation, but after the second pulse, it automatically turned to a unipolar memristor behavior. These characteristic curves are shown, respectively, in **Figures 10–13**. The operation of the memristor model as a bipolar memristor behavior is shown in **Figure 10**. The response to a bipolar with forgetting effect is shown in **Figure 11**. The response to a unipolar memristor behavior is shown in **Figure 12**. And, the memristor model response to a reversible bipolar and unipolar behavior is shown in **Figure 13**. We can conclude that our simulation results are consistent and in very good qualitative agreement with the results already published in [15]. A detailed comparison between our work model and other popular memristor models (the Chua [1], the Strukov (HP) [3], Vourkas [45], and the Chen [15]) is shown in **Table 1**. We can notice that the SPICE model gets a special advantage on describing various

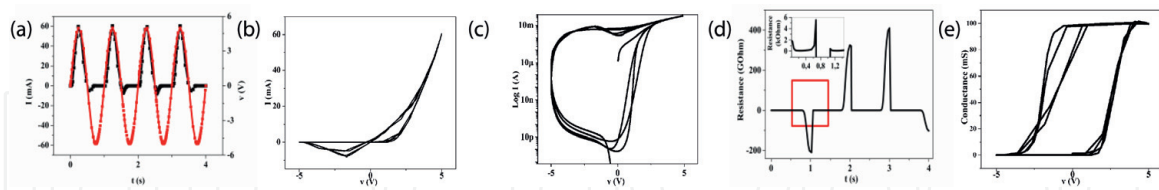


Figure 13. Memristor SPICE model response to reversible bipolar and unipolar behavior.

Memristor models	Mechanism	High frequency	Low complexity	Unipolar	Bipolar	Forgetting effect	Reversible effect	Parameters
Chua [1]	Yes	No	Yes	No	Yes	No	No	—
Strukov (HP) [3]	Yes	No	Yes	No	Yes	No	No	5
Vourkas [45]	Yes	Yes	Yes	No	Yes	No	No	12
Chen [15]	Yes	Yes	No	Yes	Yes	Yes	Yes	13
This work	Yes	Yes	Yes	Yes	Yes	Yes	Yes	13

Table 1. Comparing memristor models.

memristors models with an average number of parameters, and for its flexibility, and low complexity.

6. Conclusion

The consideration of the SPICE memristor model as a simple and flexible model was proved to explain the memristor switching, not only processing the general memristor properties, but also catching the different types of memristor behavior: the bipolar, unipolar, the bipolar with forgetting effect, and the reversible process between the bipolar and the unipolar behavior. Our simulation results demonstrate that for the bipolar memristor, a regular hysteresis curve can be obtained. For the bipolar memristor with forgetting effect, an obvious overlap between the neighbor loops of the I - V curve, and for the unipolar memristor, a positive voltage is applied, but the conductance will increase only when the voltage is over 1 V. Also, for the reversible process between bipolar and unipolar behavior, the memristor firstly behaves as a bipolar switching, and its conductance increases and decreases according to the polarity of the voltage. However, after applying a second pulse, it will turn to behave as a unipolar switching. This chapter provides a practical memristor model that can be simulated with different types of stimulus, and further studies are aimed at integrating the memristor model into a computing design with complementary metal-oxide-semiconductor (CMOS) circuits that can perform the necessary functions on a chip.

Author details


Sami Ghedira¹, Faten Ouaja Rzig^{1*}, Khaoula Mbarek¹ and Kamel Besbes^{1,2}

¹ Micro-Optoelectronics and Nanostructures Laboratory, Faculty of Sciences, University of Monastir, Tunisia

² Center for Research in Microelectronics and Nanotechnology, Technopole in Sousse, Tunisia

*Address all correspondence to: faten_ouaja@yahoo.fr

IntechOpen

© 2019 The Author(s). Licensee IntechOpen. This chapter is distributed under the terms of the Creative Commons Attribution License (<http://creativecommons.org/licenses/by/3.0>), which permits unrestricted use, distribution, and reproduction in any medium, provided the original work is properly cited. 

References

- [1] Chua L. Memristor—the missing circuit element. *IEEE Transactions on Circuit Theory*. 1971;**18**(5):507-519
- [2] Chua LO, Kang SM. Memristive devices and systems. *Proceedings of the IEEE*. 1976;**64**(2):209-223
- [3] Strukov DB, Snider GS, Stewart DR, Williams RS. The missing memristor found. *Nature*. 2008;**453**(7191):80-83
- [4] Yang JJ, Pickett MD, Li X, Ohlberg DA, Stewart DR, Williams RS. Memristive switching mechanism for metal/oxide/metal nanodevices. *Nature Nanotechnology*. 2008;**3**(7):429-433
- [5] Yang JJ, Miao F, Pickett MD, Ohlberg DA, Stewart DR, Lau CN, et al. The mechanism of electroforming of metal oxide memristive switches. *Nanotechnology*. 2009;**20**(21):215201
- [6] Sharifi MJ, Banadaki YM. General spice models for memristor and application to circuit simulation of memristor-based synapses and memory cells. *Journal of Circuits, Systems, and Computers*. 2010;**19**(02):407-424
- [7] Pickett MD. [Ph.D. thesis]. Berkeley: University of California; 2010
- [8] Jo SH, Chang T, Ebong I, Bhadviya BB, Mazumder P, Lu W. Nanoscale memristor device as synapse in neuromorphic systems. *Nano Letters*. 2010;**10**(4):1297-1301
- [9] Biolek D, Biolkova V, Biolek Z. SPICE model of memristor with nonlinear dopant drift. *Radioengineering*. 2009;**18**(2):210-214
- [10] Howard G, Bull L, de Lacy Costello B, Gale E, Adamatzky A. Evolving spiking networks with variable resistive memories. *Evolutionary Computation*. 2014;**22**(1):79-103
- [11] Yakopcic C, Taha TM, Subramanyam G, Pino RE. Generalized memristive device SPICE model and its application in circuit design. *IEEE Transactions on Computer-Aided Design of Integrated Circuits and Systems*. 2013;**32**(8):1201-1214
- [12] Nugent MA, Molter TW. AHaH computing—from metastable switches to attractors to machine learning. *PLoS One*. 2014;**9**(2):e85175
- [13] Yakopcic C. [Ph.D. thesis]. Dayton, Ohio: University of Dayton; 2011
- [14] Yakopcic C, Taha TM, Subramanyam G, Pino RE. In: *The 2013 International Joint Conference on Neural Networks (IJCNN) 2013*; IEEE, University of Dayton, Dayton; 4-9 August 2013. pp. 1-7
- [15] Chen L, Li C, Huang T, Hu X, Chen Y. The bipolar and unipolar reversible behavior on the forgetting memristor model. *Neurocomputing*. 2016;**171**: 1637-1643
- [16] <http://www.memristor.org/artificial-intelligence/124/slime-mold-periodic-timing-with-memristor-modeling>. Accessed: October 2008
- [17] Gale E, Adamatzky A, De Lacy Costello B. Slime mould memristors. *BioNanoScience*. 2015;**5**(1):1-8
- [18] Ascoli A, Tetzlaff R, Corinto F, Gilli M. In: *2013 IEEE International Symposium on Circuits and Systems (ISCAS2013)*; 19-23 May 2013; IEEE; pp. 205-208
- [19] Li Q, Serb A, Prodromakis T, Xu H. A memristor SPICE model accounting for synaptic activity dependence. *PLoS One*. 2015;**10**(3):e0120506
- [20] Biolek D, Di Ventra M, Pershin YV. Reliable SPICE simulations of

memristors, memcapacitors and meminductors. arXiv preprint arXiv: 1307.2717. 2013

[21] Pershin YV, Di Ventra M. SPICE model of memristive devices with threshold. arXiv preprint arXiv: 1204.2600. 2012

[22] Xu K, Zhang Y, Wang L, Yuan M, Joines WT, Liu QH. In: Gu M, Yuan X, Qiu M editors. ISPDI 2013-Fifth International Symposium on Photoelectronic Detection and Imaging. International Society for Optics and Photonics; 25 June 2013. pp. 89110 H-89110 H-7. Proc. of SPIE (Beijing, China)

[23] Chen L, Li C, Huang T, Chen Y, Wen S, Qi J. A synapse memristor model with forgetting effect. *Physics Letters A*. 2013;377(45):3260-3265

[24] Xu-Dong F, Yu-Hua T, Jun-Jie W. SPICE modeling of memristors with multilevel resistance states. *Chinese Physics B*. 2012;21(9):098901

[25] Abdalla H, Pickett MD. In: 2011 IEEE International Symposium of Circuits and Systems (ISCAS); 15-18 May 2011; pp. 1832-1835

[26] Singh T. Hybrid Memristor-CMOS (MeMOS) based Logic Gates and Adder Circuits. arXiv preprint arXiv: 1506.06735. 2015

[27] Kolka Z, Biolek D, Biolkova V. On steady state analysis of circuits with memristors. In: *Radioelektronika (RADIOELEKTRONIKA)*, 2011 21st International Conference IEEE; 19-20 April 2011; pp. 1-4

[28] Zaplatilek K. In: *Proceeding ECC'11 Proceedings of the 5th European conference on European Computing Conference*; 28-30 April 2011; Paris, France. pp. 62-67

[29] Mohanty SP. [Ph.D. thesis]. Denton, Texas: University of North Texas; 2013

[30] Ascoli A, Tetzlaff R, Biolek Z, Kolka Z, Biolková V, Biolek D. The art of finding accurate memristor model solutions. *IEEE Journal on Emerging and Selected Topics in Circuits and Systems*. 2015;5(2):133-142

[31] Elgabra H, Farhat IA, Al Hosani AS, Homouz D, Mohammad B. In: 2012 International Conference on Innovations in Information Technology (IIT); 18-20 March 2012; IEEE; pp. 156-161

[32] Halawani Y, Mohammad B, Homouz D, Al-Qutayri M, Saleh H. Modeling and optimization of memristor and STT-RAM based memory for low-power applications. *IEEE Transactions on Very Large Scale Integration (VLSI) Systems*. 2016;24(3): 1003-1014

[33] Yang Y, Mathew J, Shafik RA, Pradhan DK. Verilog-A based effective complementary resistive switch model for simulations and analysis. *IEEE Embedded Systems Letters*. 2014;6(1): 12-15

[34] Shahim-Aeen A, Karimi G. Triplet-based spike timing dependent plasticity (TSTDTP) modeling using VHDL-AMS. *Neurocomputing*. 2015;149:1440-1444

[35] Haase J, Lange A. Hybrid Dynamical Systems for Memristor Modelling. In: *Languages, Design Methods, and Tools for Electronic System Design*. Springer International Publishing; 2015). Volume 311 of the series Lecture Notes in Electrical Engineering, 22 August 2014. pp. 87-101

[36] Rezgui A, Gerbaud L, Delinchant B. Unified modeling technique using VHDL-AMS and software components. *Mathematics and Computers in Simulation*. 2013;90:266-276

[37] Haase J, Lange A. In: 2013 Forum on Specification and Design Languages

(FDL); 24-26 September 2013; pp. 1636-9874

[38] Mbarek K, Ouaja Rzig F, Ghedira S, Besbes K. In: 2017 International Conference on Control, Automation and Diagnosis (ICCAD); Hammamet, Tunisia; 2017. pp. 054-059

[39] Zhang L, Ge N, Yang JJ, Li Z, Williams RS, Chen Y. Low voltage two-state-variable memristor model of vacancy-drift resistive switches. *Applied Physics A: Materials Science & Processing*. 2015;119(1):1-9

[40] Oblea AS, Timilsina A, Moore D, Campbell KA. In: 2010 International Joint Conference on Neural Networks (IJCNN); 2010; pp. 1-3

[41] Miao F, Strachan JP, Yang JJ, Zhang MX, Goldfarb I, Torrezan AC, et al. Anatomy of a nanoscale conduction channel reveals the mechanism of a high performance memristor. *Advanced Materials*. 2011;23(47):5633-5640

[42] Miller KJ. [Ph.D. thesis]. Iowa State University; 2010

[43] Jo SH, Lu W. CMOS compatible nanoscale nonvolatile resistance switching memory. *Nano Letters*. 2008; 8(2):392-397

[44] Strachan JP, Torrezan AC, Medeiros-Ribeiro G, Williams RS. Measuring the switching dynamics and energy efficiency of tantalum oxide memristors. *Nanotechnology*. 2011; 22(50):505402

[45] Jeong DS, Schroeder H, Waser R. Coexistence of bipolar and unipolar resistive switching behaviors in a Pt/TiO₂/Pt stack. *Electrochemical and Solid-State Letters*. 2007;10(8):G51-G53

[46] Sun X, Li G, Zhang XA, Ding L, Zhang W. Coexistence of the bipolar and unipolar resistive switching behaviours in Au/SrTiO₃/Pt cells.

Journal of Physics D: Applied Physics. 2011;44(12):125404

[47] Vourkas I, Batsos A, Sirakoulis GC. SPICE modeling of nonlinear memristive behavior. *International Journal of Circuit Theory and Applications*. 2015;43(5):553-565

[48] Chang T, Jo SH, Lu W. Short-term memory to long-term memory transition in a nanoscale memristor. *ACS Nano*. 2011;5(9):7669-7676

[49] Lee SB, Chang SH, Yoo HK, Yoon MJ, Yang SM, Kang BS. Reversible changes between bipolar and unipolar resistance-switching phenomena in a Pt/SrTiO_x/Pt cell. *Current Applied Physics*. 2012;12(6):1515-1517

[50] Schindler C, Thermadam SCP, Waser R, Kozicki MN. Bipolar and unipolar resistive switching in Cu-Doped SiO₂. *IEEE Transactions on Electron Devices*. 2007;54(10): 2762-2768